Inorg. Chem. **2006**, *45*, 1627–1637

Metal–Organic Frameworks from Homometallic Chains of Nickel(II) and 1,4-Cyclohexanedicarboxylate Connectors: Ferrimagnet–Ferromagnet Transformation

Mohamedally Kurmoo,*,† Hitoshi Kumagai,‡ Motoko Akita-Tanaka,‡ Katsuya Inoue,‡,§ and Seishi Takagi‖

Laboratoire de Chimie de Coordination Organique, UMR7140-CNRS, Institut Le Bel, Université Louis Pasteur, 4 rue Blaise Pascal, 67000 Strasbourg Cedex, France, Applied Molecular Science, Institute for Molecular Science (IMS), Nishigounaka 38, Myoudaiji, Okazaki 444-8585, Japan, Department of Chemistry, Faculty of Science, Hiroshima University, 1-3-1 Kagamiyama, Higashi Hiroshima, Hiroshima 739-8526, Japan, and Department of Physics, Kyushu Institute of Technology, Tobata-ku, Kitakyushu 804-8550, Japan

Received September 22, 2005

The hydrothermal reactions of nickel(II) nitrate with a mixture of the geometric cis and trans isomers of 1,4-cyclohexanedicarboxylic acid (1,4-chdc or $C_6H_{10}(COOH)_2$) and a base yield three structurally different complexes, $[Ni_3(\mu^3\text{-}OH)_2(\mu^4\text{-}cis\text{-}1,4\text{-}chdc)_2(H_2O)_4]\cdot 2H_2O$ (**1**), $[Ni_3(\mu^3\text{-}OH)_2(\mu^4\text{-}trans\text{-}1,4\text{-}chdc)_2(H_2O)_4]\cdot 4H_2O$ (**2**), and $[Ni(H_2O)_4(\mu^2\text{-}trans\text{-}1,4\text{-}chdc)]$, depending on the reaction conditions. The single-crystal X-ray structure analyses of **1** and **2** reveal segregation of the isomers and formation of frameworks based on infinite $Ni_3(OH)_2(H_2O)_4$ chains, acting as secondary building units, connected by either *cis*- or *trans*-chdc for **1** and **2**, respectively. The frameworks sustain channels that house two or four water molecules, respectively, according to the size and shape of the channels that depend on the particular isomer. The structure of **3** consists of chains of square-planar $Ni(H_2O)_4$ bridged by *trans*-chdc. Magnetic data as a function of temperature and field of the virgin samples for **1** indicate long-range ordering (LRO) to a ferrimagnetic ground state at 2.1 K that is reversibly transformed into a ferromagnet below 4.4 K upon partial dehydration and rehydration. Powder X-ray diffraction of **1**, in its virgin state, after dehydration and after rehydration, confirms the stability of the framework. The magnetic data for **2** tend toward a LRO state to possibly a ferrimagnet below 2 K. The temperature dependence of the susceptibility of the two compounds is accounted for by the presence of both ferro- and antiferromagnetic exchanges within each chain via Ni–O–Ni and Ni–O–C–O–Ni pathways and weak coupling between neighboring chains via the 1,4-chdc unit. **3** is a uniform $s = 1$ antiferromagnetic chain ($J/k_B = 2.27(1)$ K).

Introduction

Among the active fields of research in contemporary chemistry and physics of materials is that dealing with metal−organic frameworks and coordination polymers, where the interests span from being purely academic, centering on different aspects of chemistry and physics, to applications such as separation, catalysis, and potential fuel-gas storage.[1] From an academic point of view, chemists are interested in understanding the structural aspects, such as coordination and hydrogen bonding and $\pi-\pi$ interactions,

* To whom correspondence should be addressed. Telephone: 00 33 3 90 24 13 56. Fax: 00 33 3 90 24 13 25. E-mail: kurmoo@chimie.u-strasbg.fr.

† Université Louis Pasteur.

‡ Institute for Molecular Science.

§ Hiroshima University.

‖ Kyushu Institute of Technology.

(1) (a) Robson, R.; Batten, S. R. *Angew. Chem., Int. Ed.* **1998**, *37*, 1460. (b) Kitagawa, S.; Kitaura, R.; Noro, S. *Angew. Chem., Int. Ed.* **2004**, *43*, 2334. (c) Eddaoudi, M.; Moler, D. B.; Li, H.; Chen, B.; Reineke, T. M.; O'Keefe, M.; Yaghi, O. M. *Acc. Chem. Res.* **2001**, *34*, 319. (d) Rao, C. N. R.; Natarajan, S.; Vaidyanathan, R. *Angew. Chem., Int. Ed.* **2004**, *43*, 1466. (e) Moulton, B.; Zaworotko, M. J.; *Chem. Rev.* **2001**, *101*, 1658. (f) Bradshaw, D.; Claridge, J. B.; Cussen, E. J.; Rosseinsky, M. J. *Acc. Chem. Res.* **2005**, *38*, 273. (g) Cheetham, A. K.; Ferey, G.; Loiseau, T. *Angew. Chem., Int. Ed.* **1999**, *38*, 3268. (h) Harrison, W. T. A. *Curr. Opin. Solid State Mater.* **2002**, *6*, 407. (i) Hagrman, P. J.; Hagrman, D.; Zubieta, J. *Angew. Chem., Int. Ed.* **1999**, *38*, 2638. (j) Maschmeyer, T.; Rey, F.; Sankar, G.; Thomas, J. M. *Nature* **1995**, *378*, 159. (k) Bu, X.; Feng, P.; Stucky, G. D. *J. Solid State Chem.* **1997**, *131*, 387. (l) Clearfield, A. *Inorganic Ion Exchange Materials*; Clearfield, A., Ed.; CRC Press: Boca Raton, FL, 1991.

10.1021/ic051633n CCC: $33.50
Published on Web 01/18/2006

and the organization of molecular bricks in the solid for the ultimate goal of predicting crystal structures and, consequently, designing synthetic approaches to materials.[2] From a different approach physical chemists and physicists are interested in studying the different functions of these materials such as electrical conductivity, magnetism, and optical properties.[3] A further aspect of these materials, which is under active research, is that dealing with porosity.[4] Synthesis and characterization of finite and infinite assemblies, employing coordination chemistry, are at the forefront in these investigations with the aim of incorporating physical functions that can be introduced by judicious choice of the metal centers and/or the organic ligands and solvents. These metal−organic hybrids, as they are often called, also present unique possibilities to combine the properties associated with the individual components, the organic and the inorganic, in the one compound with the consequent aim of controlling the communication between these individual properties.[5]

With the above aim, our ongoing program of research dealing with the search of organic−inorganic hybrid materials having dual properties has recently demonstrated a successful approach to create porous magnets.[6−8] The combination of structural properties such as porosity with magnetism is rare, and is believed to be inimical, because the requirement to stabilize magnetic long-range ordering in a material needs some orbital overlap between the nearest neighboring moment-carrying metal centers in coordinating compounds while for the creation of porosity one needs to separate these metal centers.[6−9] To overcome this difficulty, we have focused on frameworks derived from chains or layers of moment-carrying transition metals where the bonding within the chains and layers contain M−O−M connections. We have also shown the existence of magnetism in a three-dimensional (3D) framework, having M−O−M connections,[10] where the structure is based on the diamond structure consisting of tetrahedral nodes of five octahedrally coordinated MO_6 units. This approach is based on the idea that the presence of M−O−M connections will generate, through short-range exchange interactions, effective giant spins which increase in size as the temperature is lowered until they attain critical moments for them to couple by weak through-space dipolar or weak through-bond interactions to generate a 3D magnetic ordered ground state.[7,11,12] In each case we have studied, we have confirmed the porosity by reversible single-crystal to single-crystal transformation upon desolvation and resolvation using in situ diffraction.[6−8] In the series based on 3D metal formates,[8] we showed the tunability of the magnetic ordering temperatures by the nature of the inserted molecules in the cavities. On a different system based on linear chain cobalt hydroxide connected by squarate, the magnetic ground state was found to reversibly transform from an antiferromagnet to a ferromagnet upon

(2) (a) Kitagawa, S.; Kitaura, R. *Comments Inorg. Chem.* **2002**, *23*, 101. (b) Kitaura, R.; Fujimoto, K.; Noro, S.; Kondo, M.; Kitagawa, S. *Angew. Chem., Int. Ed.* **2002**, *41*, 133. (c) Barton, T. J.; Bull, L. M.; Klemperer, W. G.; Loy, D. A.; McEnaney, B.; Misono, M.; Monson, P. A.; Pez, G.; Scherer, G. W.; Vartuli, J. C.; Yaghi, O. M. *Chem. Mater*. **1999**, 2633. (d) O'Keeffe, M.; Eddaoudi, M.; Li, H.; Reineke, T.; Yaghi, O. M. *J. Solid State Chem.* **2000**, *152*, 3. (e) Kitagawa, S.; Kondo, M. *Bull. Chem. Soc. Jpn*. **1998**, *71*, 1739. (f) Biradha, K.; Hongo, Y.; Fujita, M. *Angew. Chem., Int. Ed*. **2002**, *41*, 3395. (g) Robson, R. *J. Chem. Soc. Dalton Trans.* **2000**, 3735. (h) Carlucci, L.; Ciani, G.; Proserpio, D. M.; Porta, F. *Angew. Chem., Int. Ed*. **2003**, *42*, 317. (i) Long, D. L.; Blake, A. J.; Champness, N. R.; Wilson, C.; Schroder, M.; *Angew. Chem., Int. Ed*. **2001**, *40*, 2444. (j) Seo, J. S.; Whang, D.; Lee, H.; Jun, S. I.; Oh, J.; Jeon, Y. J.; Kim, K. *Nature* **2000**, *404*, 982. (k) Robl, C. *Z. Naturforsch*. **1988**, *B43*, 993. (l) Robl, C. *Z. Anorg. Allg. Chem.* **1987**, *554*, 79. (m) Fujita, M.; Tominaga, M.; Hori, A.; Therrien, B.; *Acc. Chem. Res.* **2005**, *38*, 369.

(3) (a) Day, P., Gillespie, R., Eds. *Philos. Trans. R. Soc. London, Ser. A* **1985**, *A314*, 1. (b) *Metal-Organic and Organic Molecular Magnets*; Day, P., Underhill, A. E., Eds.; *Philos. Trans. R. Soc*. **1999**, *357*. (c) Kahn, O. *Acc. Chem. Res*. **2000**, 33, 647. (d) *Molecular Magnetism, New Magnetic Materials*; Itoh, K., Kinoshita, M., Eds.; Gordon Breach-Kodansha: Tokyo, 2000.

(4) (a) Yaghi, O. M.; O'Keefe, M.; Ockwig, N. W.; Chae, H. K.; Eddaoudi, M.; Kim, J. *Nature* **2003**, *423*, 705. (b) Eddaoudi, M.; Kim, J.; Rosi, N.; Vodak, D.; Wachter, J.; O'Keeffe, M.; Yaghi, O. *Science* **2002**, *296*, 469. (c) Rosseinsky, M. J. *Microporous Mesoporous Mater*. **2004**, *73*, 15. (d) Xu, X.; Nieuwenhuyzen, M.; James, S. L. *Angew. Chem., Int. Ed.* **2002**, *41*, 764. (e) Lee, E. Y.; Suh, M. P. *Angew. Chem., Int. Ed.* **2004**, *43*, 2798.

(5) (a) Kurmoo, M.; Graham, A. W.; Day, P.; Coles, S. J.; Hursthouse, M. B.; Caulfield, J. L.; Singleton, J.; Pratt, F. L.; Hayes, W.; Ducasse, L.; Guioneeau, P. *J. Am. Chem. Soc.* **1995**, *117*, 12209. (b) Coronado, E.; Galan-Máscarós, J. R.; Gómez-García, C. J.; Laukhin, V. *Nature* **2000**, *408*, 447. (b) Day, P.; Kurmoo, M. *J. Mater. Chem.* **1997**, *7*, 1291. (c) Fujiwara, H.; Kobayashi, H.; Fujiwara, E.; Kobayashi, A. *J. Am. Chem. Soc.* **2002**, *124*, 6816. (d) Zhang, B.; Tanaka, H.; Fujiwara, H.; Kobayashi, H.; Fujiwara, E.; Kobayashi, *A. J. Am. Chem. Soc.* **2002**, *124*, 9982. (e) Uji, S.; Shinagawa, H.; Terashima, T.; Yakabe, T.; Terai, Y.; Tokumoto, M.; Kobayashi, A.; Tanaka, H.; Kobayashi, H. *Nature* **2001**, *410*, 908. (f) Sato, O. *Acc. Chem. Res.* **2003**, *36*, 692. (g) Sunatsuki, Y.; Ikuta, Y.; Matsumoto, N.; Ohta, H.; Kojima, M.; Iijima, S.; Hayami, S.; Maeda, Y.; Kaizaki, S.; Dahan, F.; Tuchagues, J. P. *Angew. Chem., Int. Ed*. **2003**, *42*, 1614. (h) Lacroix, P. G.; Malfant, I.; Bénard, S.; Yu, P.; Rivière, E.; Nakatani, K. *Chem. Mater.* **2001**, *13*, 441. (i) Barron, L. D.; Buckingham, A. D. *Acc. Chem. Res.* **2001**, *34*, 781. (j) Inoue, K.; Kikuchi, K.; Ohba, M.; Okawa, H. *Angew. Chem., Int. Ed*. **2003**, *42*, 4810. (k) Zhang, B.; Wang, Z.-M.; Fujiwara, H.; Kobayashi, H.; Kurmoo, M.; Inoue, K.; Mori, T.; Gao, S.; Zhang, Y.; Zhu, D. *Adv. Mater.* **2005**, *17*, 1988.

(6) Kurmoo, M.; Kumagai, H.; Chapman, K. W.; Kepert, C. J. *Chem. Commun.* **2005**, 3012.

(7) (a) Kurmoo, M.; Kumagai, H.; Hughes, S. M.; Kepert, C. J. *Inorg. Chem.* **2003**, *42*, 6709. (b) Rujiwatra, A.; Kepert, C. J.; Claridge, J. B.; Rosseinsky, M. J.; Kumagai, H.; Kurmoo, M. *J. Am. Chem. Soc.* **2001**, *123*, 10584.

(8) (a) Wang, Z.-M.; Zhang, B.; Fujiwara, H.; Kobayashi, H.; Kurmoo, M. *Chem. Commun.* **2004**, 416. (b) Wang, Z.-M.; Zhang, B.; Kurmoo, M.; Green, M. A.; Fujiwara, H.; Otsuka, T.; Kobayashi, H. *Inorg. Chem.* **2005**, *44*, 1230.

(9) (a) Halder, G. J.; Kepert, C. J.; Moubaraki, B.; Murray, K. S.; Cashion, J. D. *Science* **2002**, *298*, 1762. (b) Maspoch, D.; Ruiz-Molina, D.; Wurst, K.; Domingo, N.; Cavallini, M.; Biscarini, F.; Tejada, J.; Rovira, C.; Veciana, J. *Nat. Mater.* **2003**, *2*, 190. (c) Guillou, N.; Livage, van Beek, W.; Noguès, M.; Férey, G. *Angew. Chem., Int. Ed.* **2003**, *42*, 643. (d) Beauvais, L. G.; Long, J. R. *J. Am. Chem. Soc.* **2002**, *124*, 12096. (e) Dybtsev, D. N.; Chun, H.; Yoon, S. H.; Kim, D.; Kim, K. *J. Am. Chem. Soc.* **2004**, *126*, 32. (f) Viertelhaus, M.; Adler, P.; Clérac, R.; Anson, C. E.; Powell, A. K. *Eur. J. Inorg. Chem.* **2005**, 692. (g) Forster, P. M.; Cheetham, A. K. *Angew. Chem., Int. Ed.* **2002**, *41*, 457. (h) Yang, X. D.; Si, L.; Ding, J.; Ranford, J. D.; Vittal, J. J. *Appl. Phys. Lett*. **2001**, *78*, 3502. (i) Ranford, J. D.; Vittal, J. J.; Wu, D. Q.; Yang, X. D. *Angew. Chem., Int. Ed.* **1999**, *38*, 3498. (j) Zhang, X. X.; Chui, S. S. Y.; Williams, I. D. *J. Appl. Phys.* **2000**, *87*, 6007. (k) Kahn, O.; Larionova, J.; Yakhmi, J. V. *Chem.*−Eur. J. **1999**, *5*, 3443. (l) Chavan, S. A.; Larionova, J.; Kahn, O.; Yakhmi, J. V. *Philos. Mag. B: Phys. Condens. Matter Stat. Mech. Electron. Opt. Magn. Prop.* **1998**, *77*, 1657. (m) Larionova, J.; Chavan, S. A.; Yakhmi, J. V.; Froystein, A. G.; Sletten, J.; Sourisseau, C.; Kahn, O. *Inorg. Chem.* **1997**, *36*, 6374. (n) Nakatani, K.; Bergerat, P.; Codjovi, E.; Mathoniere, C.; Yu, P.; Kahn, O. *Inorg. Chem.* **1991**, *30*, 3977.

(10) Forster P. M.; Cheetham, A. K. *Top. Catal*. **2003**, *24*, 79.

(11) (a) Kurmoo, M. *Chem. Mater*. **1999**, *11*, 3370. (b) Richard-Plouet, M.; Vilminot, S.; Guillot, M.; Kurmoo, M. *Chem. Mater.* **2002**, *14*, 3829. (c) Kurmoo, M. *J. Mater. Chem.* **1999**, *9*, 2595.

(12) (a) De'Bell, K.; MacIsaac, A. B.; Whitehead, J. P. *Rev. Mod. Phys.* **2000**, *72*, 225.

dehydration and rehydration.[6] In contrast, no change in magnetism was detected upon dehydration and rehydration of layered cobalt hydroxide connected by *trans*-1,4-cyclohexanedicarboxylate.[7]

Here, we report the synthesis, X-ray crystal structures, infrared properties, thermal properties, and magnetic properties of two complexes consisting of an identical inorganic one-dimensional backbone that is selectively connected to its nearest neighbors by one of the two geometric isomers of 1,4-cyclohexanedicarboxylate, viz., $[Ni_3(OH)_2(cis\text{-}1,4\text{-chdc})_2(H_2O)_4]\cdot 2H_2O$ (**1**) and $[Ni_3(OH)_2(trans\text{-}1,4\text{-chdc})_2(H_2O)_4]\cdot 4H_2O$ (**2**). **1** is the first example among the metal−organic frameworks to exhibit a reversible transformation from a ferrimagnetic to a ferromagnetic ground state upon dehydration and rehydration. We also report the structure and magnetic properties of a one-dimensional $s = 1$ chain $[Ni(H_2O)_4(trans\text{-}1,4\text{-chdc})]$ (**3**).

The use of flexible nonaromatic rings bearing several carboxylate groups was introduced following the interesting frameworks observed in the coordination chemistry of divalent and trivalent metals with connecting terephthalate (1,4-benzenedicarboxylate),[13] trimesate (1,3,5-benzenetricarboxylate),[14] and pyromellitate (1,2,4,5-benzenetetracarboxylate).[15] So far we have replaced the first by 1,4-cyclohexanedicarboxylate and the second by 1,3,5-cyclohexanetricarboxylate.[7,16] These two polycarboxylates provide a range of different geometric isomers, degrees of protonation of the acid, and geometries of the carboxylate in relation to the central hexane, in addition to the range of bonding capabilities of the carboxylate group already described in the literature.[17,18] Coordination polymers were reported in several reports where magnetic and nonmagnetic metals of variable charge, ranging from +1 to +3, and variable coordination numbers, ranging from 2 to 9, have been used.[7,19] Although the selectivity of geometric isomers has been reported, it is not strictly respected.

Experimental Section

Materials. All chemicals were obtained from Aldrich, Fluka, WAKO, and TCI and used as received without further purification. 1,4-Cyclohexanedicarboxylic acid is commercially available either as a mixture of 65 wt % *cis* and 35 wt % *trans* isomers or as the pure *trans* isomer.

Preparation of $[Ni_3(OH)_2(cis\text{-}1,4\text{-chdc})_2(H_2O)_4]\cdot 2H_2O$ (1). All syntheses were carried out in home-built Teflon-lined stainless steel pressure bombs of 120 mL maximum capacity. $Ni(H_2O)_6(NO_3)_2$ (1.0 g) was dissolved in distilled water (ca. 20 mL), and a solution of the neutralized mixture of *cis*- and *trans*-1,4-cyclohexanedicarboxylic acid (0.34 g) with NaOH (0.17 g) in distilled water (ca. 20 mL) was added. The mixture was placed in a Teflon-lined autoclave that was then sealed and heated to 120 °C for 3 days. It was then allowed to cool to room temperature in a cold water bath. Green needles of **1** in a clear solution were obtained. The crystals were washed with water and acetone and dried in air. Yield = 60%. Anal. Calcd (%) for **1**, $Ni_3O_{16}C_{16}H_{34}$ (formula weight (fw) = 658.5 g/mol): C, 29.18; H, 5.20. Found: C, 29.00; H, 5.27. IR (ν/cm^{-1}): 3616ms (ν OH), 3560ms (ν OH), 3380mbr (ν H_2O), 3305mbr (ν H_2O), 3125mbr (ν H_2O), 2968m, 2959m, 2942m, 2928m, 2895m, 2872m, 2850m, 1620sh (δ H_2O), 1554s (ν_{as} CO_2), 1446m, 1412s (ν_s CO_2), 1342w, 1303w, 1282w, 1270w, 1250w, 1198w, 1188w, 1144w, 1096w, 1072w, 1038w, 940w, 928w, 900w, 956w, 842w, 790w, 780w, 658w, 582w, 542w.

Preparation of $[Ni_3(OH)_2(trans\text{-}1,4\text{-chdc})_2(H_2O)_4]\cdot 4H_2O$ (2). $Ni(H_2O)_6(NO_3)_2$ (2.0 g) was dissolved in distilled water (ca. 40 mL), and a solution of the partially neutralized mixture of *cis*- and *trans*-1,4-cyclohexanedicarboxylic acid (0.59 g) with NaOH (0.13 g) was added. The resulting suspension was stirred, followed by the addition of a solution of NaOH (0.13 g). The final mixture was placed in the Teflon-lined autoclave that was then sealed and heated to 140 °C for 1 day. It was allowed to cool to room temperature in a cold water bath. Pale green cubelike crystals of **2** in a clear solution were obtained. The crystals were washed with water and acetone and dried in air. Yield = 40%. Anal. Calcd (%) for **2**, $Ni_3O_{18}C_{16}H_{38}$ (fw = 694.6 g/mol): C, 27.67; H, 5.51. Found: C, 27.35; H, 5.31. IR (ν/cm^{-1}): 3614ms (ν OH), 3560ms (ν OH), 3384mbr (ν H_2O), 3300mbr (ν H_2O), 3122mbr (ν H_2O), 2964m, 2960m, 2940m, 2924m, 2894m, 2872m, 2852m, 1625sh (δ H_2O), 1552s (ν_{as} CO_2), 1448m, 1410s (ν_s CO_2), 1340w, 1300w, 1280w, 1270w, 1250w, 1194w, 1190w, 1146w, 1094w, 1070w, 1034w, 944w, 930w, 900w, 954w, 840w, 790w, 780w, 660w, 582w, 544w.

Preparation of $[Ni(H_2O)_4(trans\text{-}1,4\text{-chdc})]$ (3). $Ni(H_2O)_6(NO_3)_2$ (1.0 g) was dissolved in distilled water (ca. 20 mL), and a solution

(13) (a) James, S. L. *Chem. Soc. Rev.* **2003**, *32*, 276. (b) Janiak, C. *J. Chem. Soc., Dalton Trans.* **2003**, 2781. (c) Janiak, C. *J. Chem. Soc., Dalton Trans.* **2000**, 3885.

(14) (a) Kepert, C. J.; Prior, T. J.; Rosseinsky, M. J. *J. Am. Chem. Soc.* **2000**, *122*, 5158. (b) Kepert, C. J.; Prior, T. J.; Rosseinsky, M. J. *J. Solid State Chem.* **2000**, *152*, 261. (c) Kepert, C. J.; Rosseinsky, M. J. *Chem. Commun.* **1998**, 31. (d) Chu, D.-Q.; Xu, J.-Q.; Duan, L.-M.; Wang, T.-G.; Tang, A.-Q.; Ye, L. *Eur. J. Inorg. Chem.* **2001**, 1135. (e) Yaghi, O. M.; Jernigan, R.; Li, H.; Davis, C. E.; Groy, T. L. *J. Chem. Soc., Dalton Trans.* **1997**, 2383. (f) Gutschke, G. O. H.; Molinier, M.; Powell, A. K.; Winpenny, R. E. P.; Wood, P. T. *Chem. Commun.* **1996**, 823. (g) Guillou, N.; Livage, C.; Marrot, J.; Ferey, G. *Acta Crystallogr.* **2000**, *C56*, 1427. (h) Livage, C.; Guillou, N.; Marrot, J.; Ferey, G. *Chem. Mater.* **2001**, *13*, 4387. (i) Foreman, M. R. S. J.; Gelbrich, T.; Hursthouse, M. B.; Platter, M. J. *Inorg. Chem. Commun.* **2000**, *3*, 234. (j) Chui, S. S.-Y.; Lo, S. M.-F.; Charmant, J. P. H.; Orpen, A. G.; Williams, I. D. *Science* **1999**, *283*, 1148. (k) Platter, M. J.; Howie, R. A.; Roberts, A. J. *Chem. Commun.* **1997**, 893. (l) Platter, M. J.; Roberts, A. J.; Marr, J.; Lachowski, E. E.; Howie, R. A. *J. Chem. Soc., Dalton Trans.* **1998**, 797. (m) Platter, M. J.; Foreman, M. R. S. J.; Coronado, E.; Gomez-Garcia, C. J.; Slawin, A. M. Z. *J. Chem. Soc., Dalton Trans.* **1999**, 4209. (n) Yaghi, O. M.; Li, H.; Groy, T. L. *J. Am. Chem. Soc.* **1996**, *118*, 9096. (o) Yaghi, O. M.; Davis, C. E.; Li, G.; Li, H. *J. Am. Chem. Soc.* **1997**, *119*, 2861. (p) Michaelides, A.; Skoulika, S.; Kirtsis, V.; Raotopoulou, C.; Terzis, A. *J. Chem. Res.* **1997**, 204.

(15) Kumagai, H.; Kepert, C. J.; Kurmoo, M. *Inorg. Chem.* **2002**, *41*, 3410 and references therein.

(16) Kumagai, H.; Akita-Tanaka, M.; Inoue, K.; Kurmoo, M. *J. Mater. Chem.* **2001**, *11*, 2146.

(17) Eliel, E. L.; Allinger, N. L.; Angyal, S. J.; Morrison, G. A. *Conformational Analysis*; John Wiley: New York, 1996.

(18) (a) Deacon, G. B.; Phillips, R. J. *Coord. Chem. Rev.* **1980**, 33, 227. (b) Mehrothra, R. C.; Bhora, R. *Metal Carboxylates*; Academic Press: New York, 1983. (c) Oldham, C. *Prog. Inorg. Chem.* **1968**, *10*, 223. (d) Doedens, R. J. *Prog. Inorg. Chem.* **1976**, *21*, 209.

(19) (a) Cotton, F. A.; Daniels, L. M.; Lin, C.; Murillo, C. A.; Yu, S.-Y. *J. Chem. Soc., Dalton Trans.* **2001**, 502. (b) Kim, J.; Jung, D. Y. *Chem. Commun.* **2002**, 908. (c) Qi, Y. J.; Wang, Y. H.; Hu, C. W.; Cao, M. H.; Mao, L.; Wang, E. B. *Inorg. Chem.* **2003**, *42*, 8519. (d) Bi, W.; Cao, R.; Sun, D.; Yuan, D.; Li, X.; Wang, Y.; Li, X.; Hong, M. *Chem. Commun.* **2004**, 2104. (e) Du, M.; Cai, H.; Zhao, X.-J. *Inorg. Chim. Acta* **2005**, *358*, 4034. (f) Inoue, M.; Atake, T.; Kawaji, H.; Tojo, T. *Solid State Commun.* **2005**, *134*, 303. (g) Nozaki Kato, C.; Hasegawa, M.; Sato, T.; Yoshizawa, A.; Inoue, T.; Mori, W. *J. Catal.* **2005**, *230*, 226. (h) Inoue, M.; Moriwaki, M.; Atake, T.; Kawaji, H.; Tojo, T.; Mori, W. *Chem. Phys. Lett.* **2002**, *365*, 509. (i) Takamizawa, S.; Mori, W.; Furihata, M.; Takeda, S.; Yamaguchi, K. *Inorg. Chim. Acta* **1998**, *283*, 268. (j) Cotton, F. A.; Lin, C.; Murillo, C. A. *Acc. Chem. Res.* **2001**, *34*, 759.

Table 1. Detail of Crystallographic Data and Refinements for Compounds **1**−**3**

	1	**2**	**3**
empirical formula	$C_{16}H_{34}Ni_3O_{16}$	$C_{16}H_{38}Ni_3O_{18}$	$C_8H_{18}NiO_8$
formula weight	658.56	694.62	300.93
T (K)	293	293	173
wavelength (Å)	0.710 73	0.710 73	0.710 73
crystal system	monoclinic	monoclinic	triclinic
space group	$P2_1/c$ (No. 14)	$C2/m$ (No. 12)	$P\bar{1}$ (No. 2)
a (Å)	6.4234(2)	20.112(3)	4.8931(7)
b (Å)	14.0681(7)	10.056(1)	6.2735(8)
c (Å)	12.669(6)	6.3805(8)	9.5319(13)
α (deg)	90	90	79.855(2)
β (deg)	91.051(5)	97.108(4)	78.971(3)
γ (deg)	90	90	77.076(7)
V (Å^3)	1144.64(54)	1280.5(3)	277.19(7)
Z	2	2	1
D_c (g cm^{-3})	1.911	1.786	1.803
μ(Mo Kα) (cm^{-1})	25.22	22.65	17.80
no. reflns	2613	1529	1615
no. params	182	91	89
R (R_w) (all data)	0.0384 (0.0673)	0.076 (0.102)	0.0247 (0.0658)
R1	0.0282 ($I > 3.00\sigma(I)$)	0.0457 ($I > 2.00\sigma(I)$)	0.0242 ($I > 2.00\sigma(I)$)
GOF	1.029	1.063	1.115
residual (e/A^3)	+0.410/−0.464	+1.09/−0.70	+0.737/−0.839

of neutralized mixed *cis*- and *trans*-1,4-cyclohexanedicarboxylic acid (0.34 g) or only the *trans* isomer (0.34 g) with NaOH (0.17 g) in distilled water (ca. 20 mL) was added. The mixture was placed in the Teflon-lined autoclave that was then sealed and heated to 100 °C for 1 day. It was then allowed to cool to room temperature in a water bath. Pale blue-green block crystals were obtained. The crystals were washed with water and acetone and dried in air. Yield = 70%. Anal. Calcd (%) for **2**, $NiO_8C_8H_{18}$ (fw = 300.9 g/mol): C, 31.93; H, 6.03. Found (%): C, 32.09; H, 5.94. IR (ν/cm^{-1}): 3432sbr (ν H_2O), 3232sbr (ν H_2O), 2970m, 2942m, 2870m, 1640w (δ H_2O), 1516s (ν_{as} CO_2), 1412s, 1352s (ν_s CO_2), 1324m, 1303m, 1292sh, 1282m, 1264m, 1216m, 1148m, 1112m, 1080m, 1048m, 976m, 932sh, 916m, 886sh, 862m, 8442m, 772m, 692m, 665m, 586m, 547m.

Single-Crystal X-ray Crystallography and Structure Solution. Single crystals were selected and glued on the tip of glass fibers. Diffraction data for **1** were then collected on a Nonius Kappa CCD diffractometer at the Service Commun de Cristallographie in Strasbourg and those for **2** were collected on a Bruker SMART APEX CCD area detector at the Institute of Molecular Science in Okazaki employing a ω scan mode. Diffraction data for two crystals of **3**, one prepared in Okazaki and the other in Strasbourg, were recorded on the two diffractometers mentioned above. Both diffractometers employ graphite monochromated Mo Kα (0.710 73 Å) radiation. The data were corrected for Lorentz and polarization effects. The structures were solved by direct methods and expanded using Fourier techniques. The non-hydrogen atoms were refined anisotropically. The final cycle of full-matrix least-squares refinement was based on number of observed reflections ($I > 3.00\sigma(I)$ for **1** and $I > 2.00\sigma(I)$ for **2** and **3**) and n variable parameters and converged (large parameter shift was σ times its estimated standard deviation) with unweighted and weighted agreement factors of $R = \sum||F_o| - |F_c||/\sum|F_o|$ and $R_w = [\sum w(|F_o| - |F_c|)^2/\sum w|F_o|^2]^{1/2}$. Details of the crystallographic work are given in Table 1 (CCDC 251822−251824).

Physical Techniques. Powder X-ray diffraction (PXRD) data were collected at room temperature using the Bragg−Brentano geometry on a Siemens D-500 equipped with Co Kα (1.789 Å) and a forward monochromator and a JEOL-JDX-3500K diffractometer employing Cu Kα (1.541 Å) with a back monochromator. Thermogravimetric analyses (20−900 °C) were performed on a SETARAM TG-DTA system at a warming rate of 5 °C/min in a constant flow of air. That of **3** was measured on a Shimatzu TG-50 at the same heating rate. Infrared spectra were recorded by transmission through fine particles of the compounds dispersed on a KBr crystal using a Mattson or a Jasco FTIR spectrometer. The temperature and field dependence of the magnetization of the complexes were measured on a Quantum Design MPMS-XL or MPMS 5S SQUID magnetometer operating in the temperature range 1.8−400 K and fields up to 50 kOe.

Results and Discussion

Synthesis. Given that the most abundant source of 1,4-cyclohexanedicarboxylic acid is a mixture of 65 wt % *cis* and 35 wt % *trans* geometric isomers, most of the syntheses use this mixture as a starting material and, consequently, this introduces the question of segregation and mixing of these isomers in the resulting compounds.[7,19] The thermodynamic stability of the various isomers and interconversion between them are well documented.[17,19] However, no information is available on their stabilities and interconversion under autogenous pressure and also under alkaline condition. The results reported in the literature on metal complexes contain both segregation and mixing, although the former appears to be dominant. Although magnetic properties are reported for some of the transition metal complexes, mostly paramagnetic behavior has been observed so far, and this is due to the lack of large exchange interactions as a consequence of the lack of M−O−M connections.[19] The only exception is the ferrimagnetic ordering observed at 60 K in the layered cobalt hydroxide ($Co^{II}_5(OH)_8$(*trans*-chdc)·$4H_2O$) pillared by the trans isomer.[7] The latter is also the only compound to display metals with a coordination number of 4.

In our work on complexes of nickel and cobalt, we also used a mixture of *cis*- and *trans*-1,4-cyclohexanedicarboxylic acid as a starting material and we find complete segregation when there are no ancillary ligands and mixing in the presence of other ligands. In the present work on nickel without ancillary ligands, segregation is observed under the conditions used for the syntheses of the complexes.[7,20]

Crystal Structures. An important observation in the series of compounds reported here is the presence of Ni−O−Ni connections that is responsible for the long-range magnetic ordering. The second key issue is that concerning the development of structures based on secondary building units (SBUs).[21] Much is known about connecting cluster SBUs by polycarboxylate into frameworks, but only a few examples exist for those with linear-chain SBUs. Here, we present two additional examples where linear chains are the SBUs connected by a flexible dicarboxylate. The basic SBU presented here is similar to that reported for $Ni_3(OH)_2(H_2O)_4$-(fumarate)$_2$·$2H_2O$, which consists of edge-sharing pairs of octahedra forming chains through connection by the apexes of a third octahedron.[22] The latter presents a long-range

(20) Kurmoo, M.; Kumagai, H. Unpublished results.
(21) Kim, J.; Chen, B.; Reineke, T. M.; Li, H.; Eddaoudi, M.; Moler, D. B.; O'Keefe, M.; Yaghi, O. M. *J. Am. Chem. Soc.* **2001**, *123*, 8239.
(22) Konar, S.; Mukherjee, P. S.; Zangrando, E.; Lloret, F.; Chaudhuri, N. R. *Angew. Chem., Int. Ed.* **2002**, *41*, 1561.

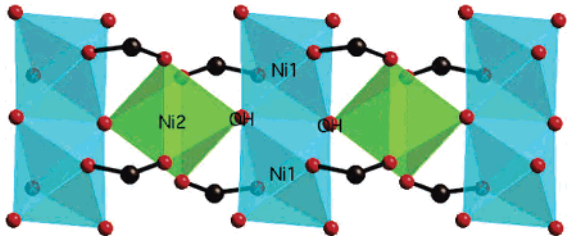

Figure 1. Part of a chain forming the secondary building unit (SBU) found in compounds **1** and **2**, showing the μ^3-hydroxide and the bridging O−C−O units of the cyclohexanedicarboxylate around the triangular arrangement of nickel atoms.

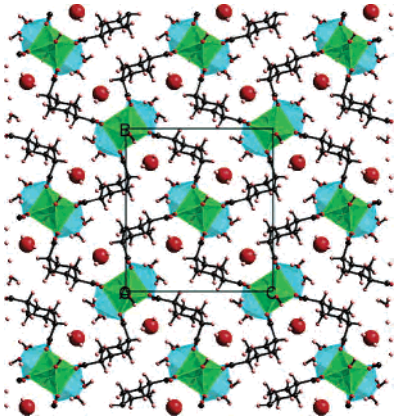

Figure 2. Projection of structure of **1** along the *a*-axis showing the *cis*-chdc connecting the one-dimensional inorganic chains in the propeller blade fashion. The polyhedra represent the Ni1 (light blue) and Ni2 (green).

magnetic ordering at 6 K. These strips may also be regarded as segments of a diagonal (110) layer of a rutile structure.[23] Two other closely related compounds are $Zn_3(OH)_2$-(dicarboxylate)$_2$·4DEF·2H_2O, where the dicarboxylate is either 4,4′-biphenyldicarboxylate or 2,6-naphthalenedicarboxylate.[24] The principal difference between these complexes is that the latter has no coordinated water molecules to the metals; consequently, the edge-sharing octahedra pair in the fumarate compound is replaced by edge-sharing tetrahedra pair in the zinc compound. The details of the crystallographic data of the compounds under study are given in Table 1.

Structure of 1. The key feature of the X-ray crystal structure of **1** is a coordination framework constructed from one-dimensional polymeric chains comprising of edge- and corner-shared octahedra of nickel acting as secondary building units (SBUs) that are connected by the flexible cyclohexanedicarboxylate. Figure 1 shows part of an inorganic chain and the coordination environment of the metal atoms, and Figure 2 shows the crystal packing viewed along the chain axis. Selected bond distances and angles are given in Table 2. The repeating unit of the chain consists of two symmetry-related Ni(1) and Ni(1′) ions and one crystallographically independent Ni(2) ion to give a triangular motif similar to that found for $Ni_3(OH)_2(H_2O)_4$(fumarate)$_2$·2H_2O.[22] Each nickel ion exhibits slightly distorted octahedral geometry comprising oxygen atoms of chdc, hydroxide, and water molecules. Ni(1) has two carboxylate oxygen atoms (O(5) and O(6)) in the *trans* positions, two bridging hydroxide oxygen atoms (O(3) and O(3′)), and two equatorial oxygen atoms from water molecules (O(1) and O(2)). The two crystallographically independent water molecules coordinate to Ni(1) in *cis* positions to complete its octahedral geometry (Figure 1). We note that the corresponding zinc atoms in the structure of $Zn_3(OH)_2$(dicarboxylate)$_2$·solvents do not have coordinated water molecules and thus adopt tetrahedral coordination geometry.[24] The coordination geometry about Ni(2), located on a crystallographic special position, is different from that of Ni(1), and it is bonded to two oxygen atoms of bridging hydroxide (O(3) and O(3′) in *trans* positions) and by four oxygen atoms of 1,4-chdc (O(4), O(4′) and O(7), O(7′), in equatorial positions). Thus, there are three different Ni(2)−O distances (Ni(2)−O(4) = 2.094 Å, Ni(2)−O(7) = 2.093 Å, Ni(2)−O(3) = 2.029 Å; Table 2). The shortest distance of Ni(2)−O(3) (2.029 Å) in relation to the other two indicates an axially compressed octahedral geometry for Ni(2). The geometry of Ni(1) is severely distorted with Ni−O distances ranging from 2.0375 to 2.109 Å. Again the Ni−OH bonds are the shortest. The hydroxide oxygen atoms (O(3)) are in *cis* positions of the Ni(1) and Ni(1′) atoms and act as μ^3-bridges between Ni(1), Ni(1′), and Ni(2). O(3) makes asymmetric Ni−O−Ni angles (Ni(1)−O(3)−Ni(1′) of 94.5° and Ni(1)−O(3)−Ni(2) of 119.8° and 122.6°); the last two are close to the tetrahedral angle required for the oxygen atom considering the presence of the hydrogen atom. Accordingly, O(3) is out of the plane defined by the three nickel atoms. These particular Ni−O−Ni angles have a considerable influence on the magnetic ground state of the compound with regard to the sign of the exchange interactions (see below). The distances between the nickel atoms are 3.520 and 3.567 Å for Ni(1)−Ni(2) and 2.995 Å for Ni(1)−Ni(1′). The triangular motif with the connected bridging hydroxide is different from that found in $M^{II}(OH)_2$.[25] The chain may be regarded as a

Table 2. Selected Bond Distances (Å) and Angles (deg) for **1**

bond	distance/Å	bond	distance/Å
Ni(1)−O(1)	2.1090(17)	Ni(1)−O(2)	2.0716(16)
Ni(1)−O(3)	2.0375(15)	Ni(1)−O(3′)	2.0406(13)
Ni(1)−O(5)	2.0697(14)	Ni(1)−O(6)	2.0928(14)
Ni(2)−O(3)	2.0288(12)	Ni(2)−O(4)	2.0944(14)
Ni(2)−O(7)	2.0930(15)		

atoms	angle/deg	atoms	angle/deg
O(1)−Ni(1)−O(2)	86.89(7)	O(1)−Ni(1)−O(3)	92.83(6)
O(1)−Ni(1)−O(3′)	176.41(7)	O(1)−Ni(1)−O(5)	91.78(7)
O(1)−Ni(1)−O(6)	84.44(7)	O(2)−Ni(1)−O(3)	175.55(7)
O(2)−Ni(1)−O(3′)	94.54(6)	O(2)−Ni(1)−O(5)	89.30(6)
O(2)−Ni(1)−O(6)	85.08(7)	O(3)−Ni(1)−O(3′)	85.49(6)
O(3)−Ni(1)−O(5)	92.52(6)	O(3)−Ni(1)−O(6)	90.48(6)
O(3)−Ni(1)−O(5′)	95.14(6)	O(3)−Ni(1)−O(6′)	92.40(6)
O(5)−Ni(1)−O(6)	172.81(6)	O(3)−Ni(2)−O(4)	85.37(5)
O(3)−Ni(2)−O(4′)	94.63(5)	O(3)−Ni(2)−O(7′)	94.50(6)
O(3)−Ni(2)−O(7)	85.50(6)	O(4)−Ni(2)−O(7)	88.06(6)
O(4)−Ni(2)−O(7′)	91.94(6)	Ni(1)−O(3)−Ni(2′)	122.60(7)
Ni(1)−O(3)−Ni(1′)	94.51(6)	Ni(1)−O(3)−Ni(2)	119.79(7)

(23) (a) Kurmoo, M.; Kumagai, H.; Green, M. A.; Lovett, B. W.; Blundell, S. J.; Ardavan, A.; Singleton, J. *J. Solid State Chem.* **2001**, *159*, 343. (b) Kurmoo, M. *Philos. Trans. R. Soc., A* **1999**, *357*, 3041.
(24) Rosi, N. L.; Eddaoudi, M.; Kim, J.; O'Keeffe, M.; Yaghi, O. M. *Angew. Chem., Int. Ed.* **2002**, *41*, 284.
(25) Zigan F.; Rothbauer. R. *Neues Jahrb. Mineral., Monatsh.* **1967**, 137.

strip of the rutile 110 layer.[23] Because Ni(2) is centered on the crystallographic special position in the monoclinic cell, the chain structure is strictly linear. However, the octahedra within the chains adopt a zigzag arrangement with a dihedral angle of 139° due to the buckling caused by the tetrahedral hydroxide oxygen with the hydrogen atoms sitting alternately on the opposite side. The chains are therefore formed by an alternation of edge-sharing pairs of octahedra and corner sharing octahedron. The chains are further stabilized by the coordination bonds of the carboxylate groups bridging the Ni(1) pairs to the Ni(2).

The four most common coordination modes of carboxylate group are shown in Scheme S1 (Supporting Information). These are (1) the carboxylate group acting as a chelating ligand to coordinate one metal, (2) the carboxylate group acting as a bidentate ligand to bridge two metal centers, (3) the carboxylate group acting as a monodentate ligand, and (4) one of the oxygen atoms acting as a bridge between two nearest-neighbor metal atoms. For the case of 2, three modes can be defined: syn−syn, syn−anti, and anti−anti. We found a stretched syn−syn of type-2 mode in our case. The Ni(1)−Ni(1′) vectors of nearest-neighbor chains are nearly orthogonal, and the shortest metal−metal distance (Ni(1)···Ni(2)) between chains is ca. 8 Å. These chains are interconnected by the flexible chdc to form the three-dimensional structure (Figure 2). They are related by a pseudo-4-fold rotation about the chain axis to give face-to-face adjacent cyclohexane rings separated by a minimum of nearly 4 Å. These chdc bridges are arranged like curved blades of a plow wheel around each chain when viewed in the direction of the chains, and they are clockwise on one chain but anticlockwise for nearest-neighboring chains. This particular arrangement results in a three-dimensional network with narrow channels along the *a*-axis housing one water molecule in the middle (otherwise two water molecules per formula unit). The approximate minimum and maximum dimensions of the channels are 4 and 13 Å (C···C distances). Water molecules in the channels are localized by weak hydrogen bonding (O···O of 2.779, 2.780, 2.841 Å or O···H of 2.012, 1.990, 2.120 Å) between coordinated water molecules and oxygen atoms of chdc.[26] However, due to the small size of the channels as well as the nearly solid walls of the channels, no interpenetration is possible. This was also noted for the zinc compounds. One of the characteristic points of the structure is the conformation of the ligand. Although a mixture of *cis* and *trans* isomers is used for the synthesis, only the *cis* form was found in this crystal structure prepared at a lower temperature, favoring a higher concentration of the *cis* form.

Dehydration and Rehydration of 1. Before presenting the X-ray data upon dehydration, it is worth discussing the thermal properties of this compound. Thermogravimetry and differential thermal analysis of **1** at a heating rate of 5 °C/min show a constant mass up to 120 °C, where it loses the mass equivalent to six molecules of water and finally decomposes to NiO between 275 and 350 °C (Figure S1).

(26) (a) Steiner, T. *Angew. Chem., Int. Ed.* **2002**, *41*, 48. (b) Desiraju, G. R. *Chem. Commun*. **2005**, 2995 and references therein.

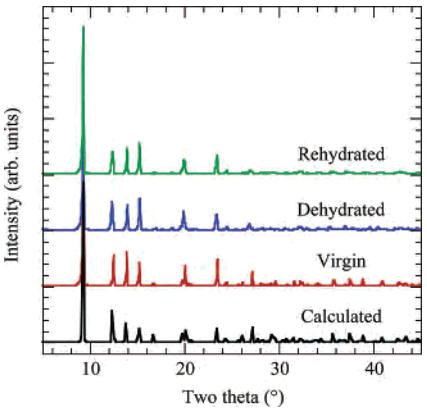

Figure 3. Powder X-ray diffraction pattern (Cu Kα) of **1** in its virgin (red), dehydrated (blue), and rehydrated (green) forms and that calculated (black) from the X-ray data of a single crystal.

To verify the stability of the crystal structure of **1** upon dehydration of only the noncoordinated water molecules, several single crystals were dehydrated in an oven at a temperature of 120 °C, which is just at the start of the dehydration process, for 24 h for X-ray data collection. In all cases, the peaks were multiple and no full structure of the dehydrated form was possible, although the cell parameters appear to be similar to those of the virgin crystal. Powder X-ray diffraction was collected for a virgin sample placed on a glass plate. The same experiment was then performed after the sample on the plate had been dehydrated for 24 h at 120 °C as well as after it had been rehydrated in the air (relative humidity 60−80%) for 1 week. The results are shown in Figure 3 as well as the calculated diffraction pattern using the single-crystal data. It is clear that the structure is not globally changed in these processes but line broadening, changes in intensity, and slight shift of the Bragg angles are observed, suggesting subtle changes in the lattice. However, severe loss of intensity and broadening at high angle prevents accurate Rietveld refinements of the data. Although we experience almost reversible magnetic properties (see below), the X-ray data suggest that the process of dehydration is not totally reversible. Further work will be needed to fully characterize the dehydrated and rehydrated forms. This problem may be associated with the lack of knowledge about the extent of dehydration as there is no plateau in the thermogravimetry between the loss of the noncoordinated and coordinated water molecules and both uncoordinated and coordinated water molecules appear to be removed at the same time at a higher temperature.

Structure of 2. The key feature of the X-ray structure of **2** is similar to that of **1**, consisting of a coordination framework constructed from polymeric chains of edge- and corner-sharing octahedra of nickel. There is one exception with respect to **1**: the *cis*-chdc is replaced by *trans*-chdc. The chain is almost identical to that of **1** as shown in Figure 1. Figure 4 shows the crystal packing viewed along the channels, and Table 3 gives some selected bond distances and angles. The chain consists of edge-sharing octahedra of two symmetry-related Ni(1) and Ni(1′) ions which are corner sharing to one crystallographically independent Ni(2) ion to give the triangular motif (Figure 1). The coordination

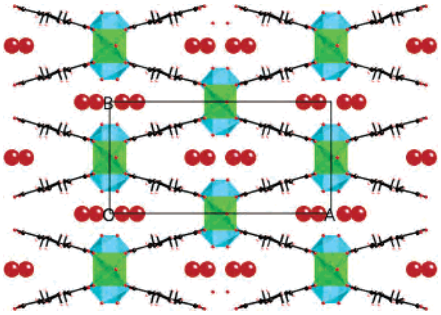

Figure 4. Projection of the structure of **2** along the *c*-axis showing the *trans*-chdc connecting the inorganic chains in linear fashion.

Table 3. Selected Bond Distances (Å) and Angles (°) for **2**

bond	distance/Å	bond	distance/Å
Ni(1)−O(1)	2.044(3)	Ni(2)−O(2)	2.083(3)
Ni(1)−O(3)	2.037(2)	Ni(2)−O(2′)	2.083(3)
Ni(1)−O(4)	2.139(3)	Ni(2)−O(3)	2.034(3)

atoms	angle/deg	atoms	angle/deg
O(1)−Ni(1)−O(1′)	172.5(2)	O(1)−Ni(1)−O(3)	95.0(1)
O(1)−Ni(1)−O(3′)	90.6(2)	O(1)−Ni(1)−O(4)	83.7(1)
O(1)−Ni(1)−O(4′)	91.0(1)	O(1′)−Ni(1)−O(3)	90.6(2)
O(1′)−Ni(1)−O(3′)	95.0(1)	O(1′)−Ni(1)−O(4)	91.0(1)
O(1′)−Ni(1)−O(4′)	83.7(1)	O(3)−Ni(1)−O(3′)	84.3(2)
O(3)−Ni(1)−O(4)	176.6(1)	O(3)−Ni(1)−O(4′)	92.5(1)
O(3′)−Ni(1)−O(4)	92.5(1)	O(3′)−Ni(1)−O(4′)	176.6(1)
O(4)−Ni(1)−O(4′)	90.6(2)	O(2)−Ni(2)−O(2′)	90.2(2)
O(2)−Ni(2)−O(2′)	180.0	O(2)−Ni(2)−O(2′)	89.8(2)
O(2)−Ni(2)−O(3)	85.4(1)	O(2)−Ni(2)−O(3′)	94.6(1)
O(2′)−Ni(2)−O(2′)	89.8(2)	O(2′)−Ni(2)−O(2′)	180.0
O(2′)−Ni(2)−O(3)	85.4(1)	O(2′)−Ni(2)−O(3′)	94.6(1)
O(2′)−Ni(2)−O(2′)	90.2(2)	O(2′)−Ni(2)−O(3′)	94.6(1)
O(2′)−Ni(2)−O(3′)	85.4(1)	O(2′)−Ni(2)−O(3)	94.6(1)
O(2′)−Ni(2)−O(3′)	85.4(1)	O(3)−Ni(2)−O(3′)	180.0
Ni(1)−O(1)−O(2′)	99.7(1)	Ni(1)−O(3)−Ni(1′)	95.7(2)
Ni(1)−O(3)−Ni(2)	120.2(1)	Ni(1)−O(3)−Ni(2′)	120.2(1)

geometry of the nickel ions in the triangular motif is similar to that found in **1**. As shown in the structure of **1**, Ni(1) and Ni(2) exhibit different coordination geometries. The shortest bond distances the Ni(2)−hydroxides (O(3) and O(3′)), indicating axially compressed octahedral geometry for Ni(2) and distorted octahedral geometry for Ni(1). The crystal of **2** belongs to the same crystal system as **1**, but in a different space group (*C*2/*m*). Consequently, both Ni(1) and Ni(2) are located on crystallographic special positions. Ni(1) has three different bond distances and Ni(2) has two different bond distances (Table 3) to exhibit a more symmetric structure than that of **1**. These chains are connected by the flexible organic moiety, chdc, to give a three-dimensional network having channels containing water molecules (Figure 4). The framework structure of **2** has two different structural features compared to **1**. One is the conformation of the 1,4-chdc and the other is the orientation of chdc and, consequently, that of the chains. All the 1,4-chdc ligands show *trans* conformation as found for $Co_5(OH)_8$(*trans*-chdc)·$4H_2O$.[7] This difference results in a change of orientation of the chains to give parallel Ni(1)−Ni(1′) vectors and, consequently, different shape and size of the channels. The approximate minimum and maximum dimensions of the channels are 4 and 20 Å (O···O distances), which are larger than those of **1**. Consequently, the water content inside the cavity is different: there are four water molecules per formula unit of **2** compared to

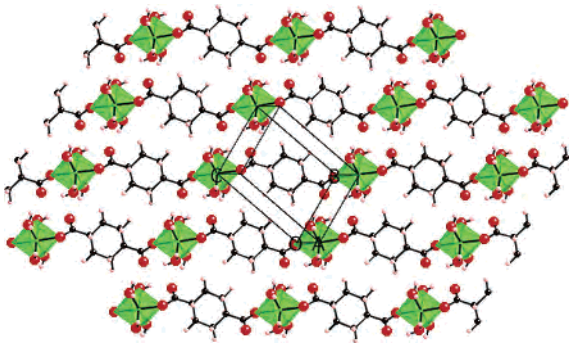

Figure 5. Structure of **3** showing the ···$Ni(H_2O)_4$−$O_2C(C_6H_{10})CO_2$−$Ni(H_2O)_4$··· chains.

only two for **1**. We should also note there is only one channel per formula unit and it contains all the water molecules in contrast to **1**, where there are two channels containing one of two molecules in each channel. The distance between the water molecules in the channels and the coordinated water molecules (O···O, 2.8 Å) indicates the presence of weak hydrogen bonding interactions. Concerning the second point, the chains are arranged parallel to one another. Similar to **1**, given that the nickel ions sit on the crystallographic special position in the monoclinic cell, the chains are strictly linear. However, the difference in space group is also a consequence of the parallel arrangement of the chains within the structure. The chdc moieties are again arranged in the form of blades around the axel of a plow wheel but are straight, not curved, due to the *trans* conformation. It is worth noting that the selectivity of the geometric *trans* isomer is consistent with the slightly higher temperature of the reaction. The Ni−O−Ni bonds angles (Ni(1)−O−Ni(2) = 119.9°, Ni(1)−O−Ni(1′) = 95.4°) with respect to the tetrahedral angles around the hydroxide oxygen atom as well as the Ni−Ni distances (Ni(1)−Ni(1) and Ni(1)−Ni(2) are 3.025 and 3.531 Å, respectively), responsible for the long-range magnetic ordering, are similar to those of **1**.

Structure of 3. The basic feature of the crystal structure of **3** is the one-dimensional chain running along the diagonal of the triclinic unit cell (Figure 5). The chain consists of square-planar $Ni^{II}(H_2O)_4$ bridged by the linear *trans*-chdc through one oxygen atom of each of the two carboxylate groups. Each carboxylate group acts as a monodentate ligand as that defined by type 3 (Scheme S1). The structure of **3** is similar to several known complexes of $M^{II}(H_2O)_4L$, where L is a linear dicarboxylate such as succinate, fumarate, and adipate.[27] The chains are parallel to one another and held together by weak hydrogen bonding. The octahedron of nickel is defined by three Ni−O distances (Table 4) due to the presence of the inversion center: two with oxygen atoms of water molecules (2.0726 and 2.0815 Å) and one with the oxygen atom of the carboxylate (2.046 Å).[26] The cyclohexane ring adopts a boat conformation with the two carboxylate

(27) (a) Gupta, M. P.; Sahu, R. D.; Ram, R.; Maulik, P. R. *Z. Kristallogr.* **1983**, *163*, 155. (b) Zheng, Y. Q.; Lin, J. L. *Z. Kristallogr.* **2000**, *215*, 159. (c) Zheng, Y. Q.; Lin, J. L. *Z. Kristallogr.* **2000**, *215*, 157. (d) Zheng, Y. Q.; Lin, J. L.; Sun, J.; Zhang, H. L. *Z. Kristallogr.* **2000**, *215*, 163. (e) Suresh, E.; Bhadbhade, M. M.; Venkatasubramanian, K. *Polyhedron* **1999**, *18*, 657. (f) Sun, D.; Cao, R.; Liang, Y.; Shi, Q.; Su, W.; Hong, M. *J. Chem. Soc., Dalton Trans.* **2001**, 2335.

Table 4. Bond Distances (Å) and Angles (deg) for **3**

bond	distance/Å	bond	distance/Å
Ni(1)−O(1)	2.0726(9)	Ni(1)−O(4)	2.0815(10)
Ni(1)−O(3)	2.0460(9)		

atoms	angle/deg	atoms	angle/deg
O(1)−Ni(1)−O(1)#1	180.0	O(3)#1−Ni(1)−O(3)	180.00(4)
O(4)#1−Ni(1)−O(4)	180.00(2)	O(1)−Ni(1)−O(4)	89.74(4)
O(3)−Ni(1)−O(1)	92.48(4)	O(3)−Ni(1)−O(1)#1	87.52(4)
O(3)−Ni(1)−O(4)	90.70(4)	O(3)−Ni(1)−O(4)#1	89.30(4)
O(1)−Ni(1)−O(4)#1	90.26(4)	O(1)#1−Ni(1)−O(4)	90.26(4)

groups parallel to each other but out of the mean plane of the hexane ring. Several hydrogen bonds exist within the structure that contribute to the stability of the complex; the shortest is within a single chain where the dangling oxygen atom of the carboxylate is at a distance of 1.795 Å to the hydrogen atom of a coordinated water molecule or 2.628 Å to the oxygen of the water molecule.[26] The second shortest distance is 2.085 Å between the coordinated oxygen atom of the carboxylate on one chain and the hydrogen atom of a water molecule of neighboring chain, or 2.858 Å between the two oxygen atoms. The shortest oxygen−cyclohexane hydrogen atom distance is 2.67 Å.

Magnetic Properties. (a) General Comments. Variable-temperature magnetization measurements have been performed on carefully chosen crystals of **1** and **2** under a microscope in the temperature range 1.8−400 K in both ac and dc mode and field dependence at several temperatures in fields up to 50 kOe. Furthermore, we have studied the in situ magnetic properties of **1** during the partial dehydration process and its rehydration. Since most extensive measurements were performed for **1**, we will first present its magnetic properties in all its different forms and then those of **2** and **3**.

For the study of the magnetic properties of **1** the following protocol was adopted. A sample was prepared from crystals carefully selected under a microscope and placed in a gelatin capsule inside a clear drinking straw. The sample was first measured in ac and dc modes on cooling in a small field of 1 Oe. The measurements were followed by those of the hysteresis loops at several temperatures below 50 K. The susceptibility was then measured in 100 Oe on warming from 2 to 400 K. At 400 K, the sample was kept for 2 h in a constant flow of helium to produce the partially dehydrated form before starting the measurements on cooling (400−2 K) in the same field (see Figures 6−8). The isothermal magnetization of the dehydrated form was then measured at several temperatures. Finally, the measurements in 1 Oe were performed following field cooling also in 1 Oe from 50 K. Following this series of measurements, the sample was allowed to stand in air for 3 weeks to be rehydrated and the same procedure was followed. The results were found to be close to those of the virgin sample and were not 100% reversible (Figure 7).

Temperature dependence of the susceptibility of **1** shows a continuous increase on lowering the temperature of the sample. However, that of the product of the magnetic susceptibility and temperature in its virgin state (Figure 6)

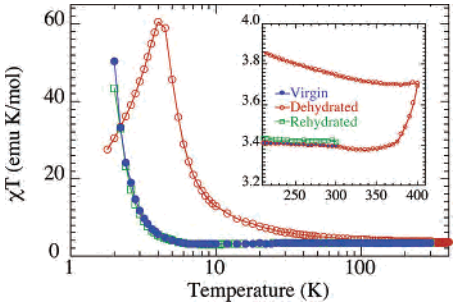

Figure 6. Temperature dependence of χT of **1** in its virgin state (blue filled circles), after partial dehydration (red open circles), and after rehydration (green squares). The inset shows an expanded view of the high-temperature region showing the increase of moment upon partial dehydration.

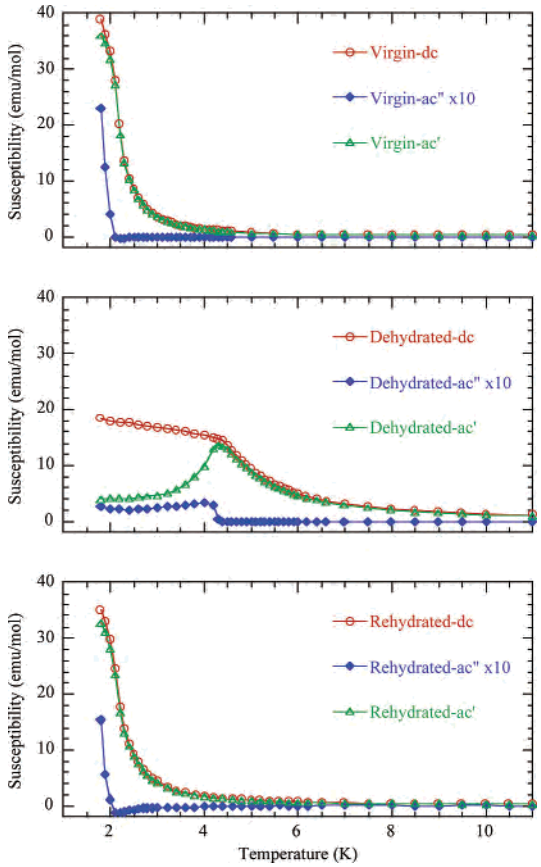

Figure 7. Temperature dependence of dc (red) and ac (blue, green; filled and open symbols for real and imaginary components, respectively) magnetizations measured in an applied field of 1 Oe for a sample of **1** in its virgin (top), partially dehydrated (middle), and rehydrated (bottom) forms.

shows some features: first, an increase on lowering the temperature to ca. 40 K, followed by a decrease to a minimum around 9 K and a very sharp increase to a maximum at 2.3 K. The results of the analysis of the data above 100 K to the Curie−Weiss law is temperature-range independent and gives a Curie constant of 3.360(1) cm^3 K mol^{-1}, consistent with three $s = 1$ Ni ions having a g-value of 2.117, and a Weiss constant of +3.14(4) K.[28] Below 40 K, the χT value drops slightly to 9 K, and it increases dramatically below 9 K to a peak at 2.3 K. Data measured in a field of 1

(28) Herpin, A. *Theorie du Magnétisme*; Presse Universitaire de France: Paris, 1968.

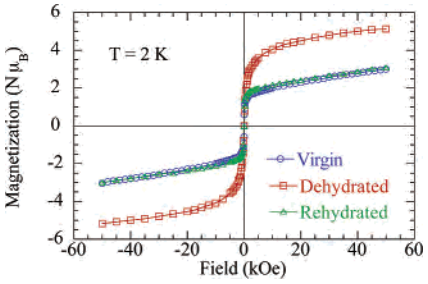

Figure 8. Isothermal magnetization of **1** at 2 K in its virgin (blue circles), partially dehydrated (red squares), and rehydrated (green triangles) forms.

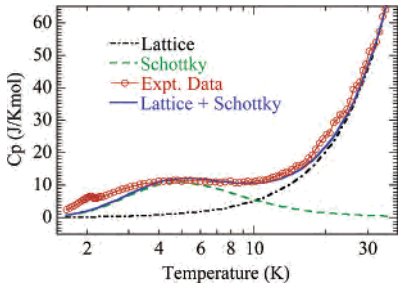

Figure 9. Observed heat capacity (circles) and estimated contributions due to Schottky (green dashed line), lattice phonons plus low-dimensional magnetic fluctuation (black dotted−dashed line), and the sum of the two (blue solid line).

Oe show the rapid increase in magnetization below 9 K in both ac and dc modes. In addition, the ac susceptibilities are accompanied by the observation of a nonzero imaginary component below 2.1 K, indicating the presence of long-range ordering (LRO). Isothermal magnetization at different temperatures confirms the transition below 2.1 K. It shows enhanced paramagnetism below 5 K, turning into a square-shaped loop at 2 K. There is very little hysteresis, suggesting that the material is a soft magnet.[29] The magnetization in 50 kOe is 3 μ_B, which is only half the value if all the moments were parallel and 1.5 times that if the moments of the two Ni(1) were antiparallel to those of Ni(2). Heat capacity has been recorded as a function of temperature, employing a pseudoadiabatic technique, in the range 1.5−40 K (see discussion below and Figure 9).

On partial dehydration of the sample at 400 K in a helium flow, a steady state is reproducibly obtained with a magnetic susceptibility slightly higher than the virgin sample (Figure 6). In contrast to that of the virgin sample, the temperature dependence of χT continuously increases on lowering the temperature until a sharp peak is found at 5 K without any other anomaly. Analysis of the data above 100 K gives $C =$ 3.531(2) cm^3 K mol^{-1} and $\theta = +17.7(1)$ K. Both values are higher than those of the virgin sample. The dc magnetization in a field of 1 Oe increases smoothly to a plateau at 4.5 K, suggesting that there is an increase of correlation length within the chains reaching nearly the maximum moment before long-range order sets in (Figure 7). The ac susceptibilities confirm the presence of LRO at 4.5 K with a peak in the real part and a nonzero imaginary part starting at 4.5 K. The isothermal magnetizations at 10, 5, and 2 K show that at 10 K the compound is paramagnetic, while at 5 K it is like a superparamagnet and at 2 K the hysteresis is consistent with that of a ferromagnet with a saturation magnetization (5.2 μ_B) approaching that of three parallel Ni moments (Figure 8).[28,29]

By allowing the sample to stand in air for 3 weeks, it almost recovers to the original state and the magnetic properties are nearly the same as those observed for the virgin sample. The temperature dependence of χT again shows the peak at around 40 K and the minimum at 9 K. Analysis of the data above 100 K gives $C = 3.391(2)$ cm^3 K mol^{-1} and $\theta = +2.5(1)$ K. The ac susceptibilities show the transition at 2.1 K. The isothermal magnetization at 2 K is identical, within experimental errors, to that of the virgin sample. We should also note that the above observations have been made on three different samples and the measurement cycles have been performed twice reproducibly on one sample.

(b) Heat Capacity of 1. The experimental heat capacity of a virgin sample of **1** is shown in Figure 9. It has three contributions: one can be regarded as coming from the lattice phonons resulting in the steep rise above 10 K, the second is the broad hump due to the Schottky term derived from the zero-field splitting of Ni(II), $s = 1$, and the third is the sharp peak at 2 K confirming the long-range magnetic ordering. The second term is easier to estimate. We estimated the Schottky anomaly by adjusting D to +13 K in the fitting procedure.[30] However, the phonon contribution is more difficult to estimate, as we find that it does not fit the usual T^3 dependence, suggesting that there may be short-range magnetic effects which prevent a reasonable fit from being obtained. We, therefore, consider the one-dimensional structure, and we analytically estimated the background by $aT^2 + bT^3$, where the former accounts for the short-range correlations due to the low dimensionality of the compound and the latter for the lattice contribution.[31] A much better fit was obtained, as shown in Figure 9. However, the magnetic entropy of the compound is distributed between short-range and long-range ordering; consequently, only a fraction of the 3D contribution is observed. The presence of the latter is important to confirm the 3D long-range ordering which is not permitted in one-dimensional antiferromagnetic magnetic chains or single chain magnets.[32]

(c) Magnetic Properties of 2. The virgin sample of **2** behaves in a way similar to that of **1** (Figures S3 and S4). It is paramagnetic in the high-temperature region with a Curie constant of 3.296(3) cm^{3}K mol^{-1} and a Weiss constant of

(29) (a) Chikazumi, S. *Physics of Ferromagnetism*; Oxford University Press: Oxford, 1992. (b) Bertotti, G. *Hysteresis in Magnetism*, Academic Press: London, 1998.

(30) Carlin, R. L. *Magnetochemistry*; Springer-Verlag: Berlin, 1986; p 45.

(31) (a) Stanley, H. E. *Introduction to Phase Transitions and Critical Phenomena*; Clarendon Press: Oxford, 1991. (b) *Magnetic Properties of Layered Transition Metal Compounds*; De Jongh, L. J., Ed.; Kluwer Academic Publishers: Dordrecht, 1990.

(32) (a) Kajiwara, T.; Nakano, M.; Kaneko, Y.; Takaishi, S.; Ito, T.; Yamashita, M.; Igashira-Kamiyama, A.; Nojiri, H.; Ono, Y.; Kojima, N. *J. Am. Chem. Soc.* **2005**, *127*, 10150 (b) Clérac, R.; Miyasaka, H.; Yamashita, M.; Coulon, C. *J. Am. Chem. Soc.* **2002**, *124*, 12837. (c) Ferbinteanu, M.; Miyasaka, H.; Wernsdorfer, W.; Nakata, K.; Sugiura, K.-i.; Yamashita, M.; Coulon, C.; Clérac, R. *J. Am. Chem. Soc.* **2005**, *127*, 3090. (d) Bogani, L.; Sangregorio, R.; Sessoli, R.; Gatteschi, D. *Angew. Chem., Int. Ed.* **2005**, *44*, 5817. (e) Gatteschi, D.; Sessoli, R. *Angew. Chem., Int. Ed.* **2003**, *42*, 268.

Table 5. Comparative Summary of Magnetic Data for **1** in All Its Forms and of **2**

compound	**1**, virgin	**1**, dehydrated	**1**, rehydrated	**2**, virgin
C (cm^3 K mol^{-1})	3.360(7)	3.531(2)	3.391(2)	3.296(4)
Θ (K)	+3.14(4)	+17.69(9)	+2.52(10)	+6.82(18)
T_{min} of χT (K)	9	no minimum	9	7.5
M_s (N μ_B) at 2 K	3	5.2	3	4

+6.8(2) K. The maximum and minimum in the χT versus T occur at 40 and 7.5 K, respectively. However, the ac susceptibility data do not reveal any transition down to the lowest temperature of 2 K of our SQUID magnetometer. The χT value of **2** at 2 K is much lower than that of **1**, which may indicate that the transition is at lower temperatures. The isothermal magnetizations at different temperatures are similar to those of the virgin sample of **1**. There is no hysteresis and the magnetization reaches 4 μ_B in a field of 50 kOe at 2 K. This value is slightly higher than that of **1** and is again lower than that expected for a ferromagnetic arrangement of the moments and higher than that expected for a ferrimagnetic alignment. Further work at lower temperatures would be needed to properly define the ground state of this compound. A canted-antiferromagnetic state cannot be excluded, though the estimated canting angle of nearly 20° appears unrealistic. This difference in magnetic properties between **1** and **2** may be associated with the large cavity of **2** that makes interchain magnetic interaction weak as well as the possible motion of the water molecules that prevent us from observing their hydrogen atoms.

The temperature dependence of the susceptibility of **1** and **2** suggests that ferromagnetic coupling dominates the high-temperature region (Table 5). This may be associated with the Ni(1) and Ni(1′) pair as a consequence of the edge-sharing short distance (2.995 and 3.025 Å, respectively) and low Ni(1)−O−Ni(1′) angle (94.5° and 95.4°, respectively) which as expected within the Goodenough−Kanamori rule is ferromagnetic.[33] At temperatures below 40 K, weak antiferromagnetic coupling between Ni(1) and Ni(2) becomes operative as $J_{(Ni(1)-Ni(2))} \geq kT$ and thus the susceptibility decreases to a minimum as expected for a ferrimagnet, since there are two ferromagnetically coupled Ni moments opposing one antiferromagnetically. We should, therefore, point out that these compounds are rare occasions of the observation of ferrimagnetism in homometallic systems.[22,34] Below the minimum at ca. 8 K, the correlation length within the chain increases as the temperature is lowered until the effective moment within each chain becomes large enough to couple to their neighbors via weak coupling through bonds or weak dipolar field through space to give a ferrimagnetic ground state. We should also note for comparison that the magnetic properties of $Ni_3(OH)_2(H_2O)_4(fumarate)_2 \cdot 2H_2O$ are also consistent with those of a ferrimagnet at 6 K.[22] In **1** the critical temperature is 2.1 K, while it appears to be lower than 2 K for **2**. The low critical temperatures compared to

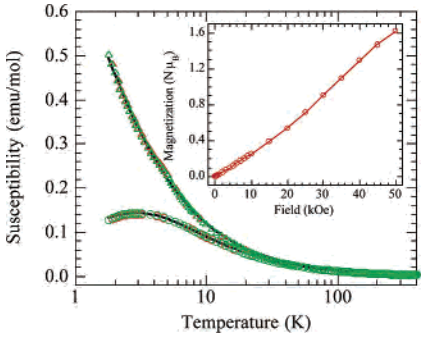

Figure 10. Temperature dependence of ac and dc susceptibility (red and green, respectively) of the virgin sample of **3** (circles) and those after it has been subjected to partial dehydration in situ. The black lines are fits to the data with a $s = 1$ one-dimensional chain for the virgin sample and a Curie−Weiss law for the dehydrated sample. Inset: isothermal magnetization at 2 K for a virgin sample.

the fumarate compound may be due to the six-atom cyclohexane bridges with only single bonds in contrast to the four carbon-atom bridges with one central double bond. However, we are currently unable to comment on the mechanism of the transformation of the magnetic ground state upon partial dehydration due to the lack of a crystal structure of the dehydrated form. With the available results, we can only speculate that dehydration results in breaking the weak interaction between the chains (the hydrogen bonds of the water molecules and the framework) in such a way that the antiferromagnetic coupling between Ni(1) and Ni(2) becomes weakly ferromagnetic.

The magnetic properties of **3**, in contrast to **1** and **2**, are much simpler (Figure 10). It behaves as a Curie−Weiss paramagnet in the range 5−300 K with a Curie constant of 1.253(8) cm^3 K mol^{-1}, corresponding to a g-value of 2.239 for $s = 1$, and a Weiss temperature of −4.23(8) K, suggesting weak antiferromagnetic coupling between nearest nickel centers through the cyclohexanedicarboxylate bridges. It deviates from this behavior below 10 K. The temperature dependence of the real part of the ac susceptibilities at low temperatures is exactly that of the dc susceptibility within experimental error. They exhibit a broad maximum at around 3 K. The data can be fitted to the model of an $s = 1$ uniform antiferromagnetic chain, also known as a Haldane chain, with an exchange coupling of J/k_B of 2.27(1) K and a g-value of 2.210(4).[35] By comparison to what is known in the literature,[36] we can conclude that the magnitude of the exchange interaction through this eight-atom bridge is quite remarkable. Further low-temperature physics of such a system with an expected low-energy Haldane gap is quite appealing and is envisaged. To check the nature of the uniform chain antiferromagnetism, we partly removed some of the water molecules by heating at 390 K (below the decomposition temperature; see Figure S2) for 1 h in the flow of helium in the SQUID magnetometer to perturb the uniformity of the chain.[37] This procedure causes the crystals to turn slightly

(33) (a) Goodenough, J. B. *Magnetism and the Chemical Bond*; John Wiley and Sons: New York, 1963. (b) Kanamori, J. *J. Phys. Chem. Solids* **1959**, *10*, 87. (c) Kanamori, J. In *Magnetism*; Rado, G. T., Suhl, H., Eds.; Academic Press: New York, 1963; Vol. I, Chapter 4, p 127.
(34) Li, J.-T.; Tao, J.; Huang, R. B.; Zheng, L.-S.; Yuen, T.; Lin, C. L.; Varughese, P.; Li, J. *Inorg. Chem.* **2005**, *44*, 4448.
(35) (a) Meyers, A.; Gleizes, A.; Girerd, J. J.; Verdaguer, M.; Kahn, O, *Inorg. Chem.* **1982**, *21*, 1729. (b) Sandvik, A. W.; Kurkijärvi, J. *Phys. Rev. B* **1991**, *43*, 5950.
(36) (a) Katsumata, K. *High Magn. Fields* **2003**, *2*, 171. (b) Yamashita, M.; Ishii, T.; Matsuzaka, M. *Coord. Chem. Rev.* **2000**, *198*, 347. (c) Katsumata, K. *J. Magn. Magn. Mater.* **1995**, *140*, 1595.

yellow and causes minor changes in the PXRD pattern but retains the global structure (Figure S5). The resulting magnetic susceptibility consequently does not show any anomaly, and it can be fitted by the Curie−Weiss law with a Curie constant of 1.298(8) cm^3 K mol^{-1} corresponding to a value of $g = 2.279$ for $s = 1$ and a very weak antiferromagnetic coupling with a Weiss constant of −0.82(3) K. Isothermal magnetization of the virgin sample at 2 K shows the linear dependence as a function of applied field reaching 1.7 μ_B in field of 50 kOe (Figure 10), which is consistent with the presence of a antiferromagnetically coupled linear chain.

Conclusion

The hydrothermal reaction of Ni(II) and mixtures of geometric isomers of 1,4-cyclohexanedicaboxylate results in total segregation in the solids based on a common $Ni_3(OH)_2$ linear chain secondary building unit connected by the fully deprotonated acid to form 3D frameworks with channels containing water molecules. Both are magnetic at low temperatures and one is found to display a reversible transformation from a ferrimagnet to a ferromagnet upon partial dehydration and rehydration, adding to the list of unusual examples of porous magnets. An estimate of the magnitude of the magnetic exchange through the chdc unit was made possible by the study of the one-dimensional antiferromagnetic chain compound, $Ni(H_2O)_4$(*trans*-chdc), obtained under different conditions. The presence of tunability and reversibility of the magnetic properties upon the presence or nature of the guest content of metal−organic frameworks enhances their potential for applications beyond those of the porous metal oxide materials.[38]

Acknowledgment. This work was funded by the CNRS, France, and JSPS and Ministry of Education, Japan. H.K. thanks the JSPS for a Young Scientists Fellowship, and M.K. thanks the Kyushu Institute of Technology for a fellowship. We also thank Drs A. Decian and N. Gruber-Kyritsakas from the X-ray facilities in Strasbourg.

Supporting Information Available: Modes of coordination of the CO group; various data for **1**, **2**, and **3**; X-ray crystallographic data. This material is available free of charge via the Internet at http://pubs.acs.org.

IC051633N

(37) (a) Yoshida, M.; Shiraki, K.; Okubo, S.; Ohta, H.; Ito, T.; Takagi, H.; Kaburagi, M.; Ajiro, Y. *Phys. Rev. Lett.* **2005**, *95*, 117202/1. (b) Takayama, H. *J. Phys. Soc. Jpn.* **2005**, *74*, 1127.

(38) (a) Davis, M. E. *Nature* **2002**, *417*, 813. (b) Garney, T. R. *Curr. Opin. Solid State Mater. Sci.* **1995**, *1*, 69. (c) Zhao, D.; Feng, J.; Huo, Q.; Melosh, N.; Fredrickson, G. H.; Chmelka, B. F.; Stucky, G. D. *Science* **1998**, *279*, 548. (d) Hare, D. O.; Walton, R. I.; Smith, R. I. *Microporous Mesoporous Mater.* **2001**, *48*, 79. (e) Lewis, D. W.; Sankar, G.; Wyles, J. K.; Thomas, J. M.; Catlow, C. R. A.; Willock, D. J. *Angew. Chem., Int. Ed. Engl.* **1997**, *36*, 2675.